

# An Approximate Solution for Heat Transfer in the Entrance Region of Laminar Newtonian Pipe Flow

GENNARO CUCCURULLO<sup>1</sup>, CARMELA CONCILIO<sup>1</sup>, DOMENICO ROSSI<sup>2</sup>,  
CLAUDIO GUARNACCIA<sup>2</sup>

<sup>1</sup>Department of Industrial Engineering,  
University of Salerno,  
Via Giovanni Paolo II, 132, Fisciano, I-84084,  
ITALY

<sup>2</sup>Department of Civil Engineering,  
University of Salerno,  
Via Giovanni Paolo II, 132, Fisciano, I-84084,  
ITALY

*Abstract:* - The study of the simultaneously developing pipe flow requires facing nonlinear systems of partial differential equations. In this framework, the aim of this paper is to demonstrate that the integral method can be an effective procedure to obtain analytic-approximate solutions that are easy to handle while allowing the recovery of a satisfactory accordance with the exact solution. To prove the above statement this paper will present a comparison between the approximate solution and the corresponding numerical solution in the entrance region of Newtonian pipe flow. Third-kind thermal boundary conditions are included, while velocity and temperature profiles at the inlet are assumed uniform. Numerical results demonstrate that the proposed approximate solution is quite accurate and readily implemented, both in terms of developing velocity and temperature profiles. Moreover, the expected functional dependence on the main parameters of the problem at hand is retained. As a consequence, the developing Fanning friction coefficient and Nusselt curves are satisfactory and accurate for different thermal boundary conditions at the wall.

*Key-Words:* - Simultaneously developing pipe flow, Newtonian pipe flow, integral method, entrance region, weighted residuals, Analytic-approximate solutions, Third-kind thermal boundary conditions, Fanning friction coefficient, Nusselt curves, Nusselt-Graetz Problem.

Received: May 23, 2024. Revised: September 7, 2024. Accepted: November 9, 2024. Published: December 11, 2024.

## 1 Introduction

Most realistic systems of ordinary differential equations do not have exact analytic solutions, so approximation or numerical techniques must be used. Numeric solutions of the Navier-Stokes equations are extremely time-consuming, while integral schemes to solve the boundary layer equations are simple to treat and practically most often used: the schemes by Pohlhausen and v. Karman are much studied, that turning in reduced efforts required for computing time as well as for low memory consumption. The Kármán–Pohlhausen (KP) momentum-integral approach, introduced in [1] and [2], is widely used in boundary-layer analysis, [3], [4], [5], [6], [7]. Its popularity relies on its effectiveness in providing a wealth of useful details for boundary layers in both low and high Reynolds number flows, [8], [9], [10].

Despite its simplicity, the KP approach continues to play a pivotal role in several monographs that devote themselves to boundary-layer theory, [11].

In this context, the aim of this study is to extend the use of the integral method having in mind several processing operations where fluids are forced through short, confined channels, [12], [13]. In situations like this one, velocity and temperature profiles are still developing without reaching the respective asymptotic shapes. Therefore, viscous shear and heat transfer rates at the wall turn out to be greater than the respective fully developed values. Heat transfer in simultaneously developing flow has to be solved essentially by numerical methods: available solutions for Newtonian fluids are summarized in [14], while a wide treatment for non-Newtonian fluids can be found in [15], [16], [17]. Besides these seminal contributions, other applications are available in the Literature,

involving a plethora of applications. In [18], as an example, the authors investigated the heat transfer of both Newtonian and Non-Newtonian flow in a tube in tube shape the mean of the Numerical approach. In [19], authors investigated the heat transfer phenomena of a more peculiar shape, also validating the numerical model with experiments. In [20], the numerical approach was pursued to study heat transfer in an artery in Newtonian and Non-Newtonian conditions, so to investigate heat phenomena in blood circulation.

In this framework, the integral method is particularly valuable as a tool for scientists and applied mathematicians. This method performs conservation of mass, momentum, and energy across the boundary-layer thickness with a given differential element in the  $x$ - direction instead of performing mass, momentum, and energy balances through a differential fluid element inside the boundary layer, as with the similarity method, the integral method. It should be reiterated for fluids with a Prandtl number different from unity, such as gases, water, and oils, the hydrodynamic boundary-layer thickness is different from the thermal boundary layer, [21]. For this reason, particular care was given to the choice for the appropriate profile.

In this paper, the approximate method is implemented to derive approximate solutions to the Navier Stokes systems of partial differential equations. It is important to underline how, despite the undeniable advantages of the integral methods, the quality of the achieved results depends on the assumption of the chosen basic profiles. The goal of obtaining a solution that is both simple and accurate is achieved through an appropriate selection of the basic shape functions, which must consider all information relevant to the problem under study, with particular reference to the limiting cases, namely the asymptotic solutions in the regions near the entrance and those that are fully developed. As a final remark of this contribution, to assess the accuracy of the approximate solution, a numerical comparison with the Finite Element Method (FEM) was carried out with commercial software. Ultimately, the results showed that the approximate analytical method can be considered a valid alternative to the classical methods available in the literature, in order to obtain accurate results that preserve the functional dependence of more elaborate solutions.

## 2 Analysis of the Method

In the present study, velocity and temperature fields are derived as approximate analytical solutions by

using the integral approach. The flow is assumed to be at a steady state for a Newtonian fluid in incompressible laminar pipe flow in the entrance region. The developing velocity flow problem cannot be strictly considered a boundary layer problem, as the axial diffusion of momentum and the radial pressure gradient are not negligible very close to the inlet. Despite this, the boundary layer approach provides a good approximation for the velocity field and significantly simplifies the momentum equations, [22]. Therefore, assuming a flow with a large Reynolds number, the simplifications from boundary layer theory are applied in the following scheme.

The boundary conditions at the tube inlet provide uniform velocity and temperature profiles. The thermal condition at the wall is of heat flux linearly depending on the wall temperature, thereby allowing for the recovery of both constant wall temperature and heat flux as limiting cases.

To overcome the difficulty connected with heavy numerical computations and to have a simple and handful solution, analytical approximate methods can be applied. The developing velocity and temperature profiles are obtained using the integral method, [23], [24], [25], which garners particular attention due to its ease of implementation and lower computational cost compared to the FEM. This makes it an attractive option when a fast solution is needed to provide quick insights or estimates of the problem at hand, such as in the case of a preliminary engineering approach. Additionally, the integral method reduces the problem to a more manageable form, maintaining the functional dependence of the solution on key parameters, provided that the basic profiles are selected appropriately. Often, as will be demonstrated, it facilitates closed-form solutions or expressions that yield more direct physical insights into the system's behaviour. Furthermore, FEM's high sensitivity to mesh quality can affect both the accuracy and stability of the solution, which underscores the robustness of the integral method in certain contexts.

In the subsequent analysis, the unknown velocity profile is represented as an expansion in terms of a similarity variable, which incorporates both the radial and axial spatial coordinates as independent variables. This choice seems suitable since both the Leveque solution near the inlet and the fully developed solution are recovered, as will be demonstrated later. To explicitly derive the unknown velocity shape functions, the integral form of the mass and momentum conservation equations is employed in conjunction with an additional

equation: the momentum equation weighted by the similarity variable. These ordinary differential equations involve only the axial variable as the independent variable. They constitute a system of two differential equations with two unknowns, which can be readily solved numerically to characterize the fundamental shape functions and, consequently, the velocity profile and axial pressure gradient.

Following a similar approach, to explicitly derive the unknown temperature shape functions, a set of two first-order differential equations is employed: the first is the integral energy balance equation, and the second is derived from the first by applying the moment method, with the similarity variable used as the weight function. Then, the calculation of the wall heat transfer is enabled.

Results are presented and discussed in dimensionless form, both in terms of the wall friction factor and the Nusselt number, for selected Biot and Prandtl numbers.

### 3 Basic Equations

To predict the fluid flow and wall heat transfer in a circular pipe, a two-dimensional axisymmetric model is employed. The velocity and temperature fields in the entrance region for incompressible, steady-state laminar flow, are determined by neglecting axial diffusion, assuming constant properties and no thermal energy sources. Uniform inlet profiles are considered, and Newtonian behaviour is assumed.

#### 3.1 Velocity Field

The mass and momentum equations and the related boundary conditions can be written in dimensionless form as:

$$r u_x + (v r)_r = 0 \quad (1)$$

$$u u_x + v u_r = -p_x + (r u_r)_r / r \quad (2)$$

$$v(x,1) = 0; v(0,r) = 0 \quad (3)$$

$$u(x,1) = 0; u(0,r) = 1; u_r(x,0) = 0 \quad (4)$$

The dimensionless variables are:

$$\begin{aligned} x &= X / R_0 / Re_R; r = R / R_0; u = U / U_0; \\ v &= V / U_0 Re_R; p = P / (\rho U_0^2); \\ Re_R &= (\rho U_0 R_0) / \mu \end{aligned} \quad (5)$$

where:  $X$  and  $R$  are the axial and the radial coordinates;  $U$  and  $V$  the axial and radial velocity components;  $P$  the pressure;  $R_0$  the tube radius;  $U_0$  the inlet velocity,  $\rho$  the density;  $\mu$  the viscosity. The

lower-case symbols indicate the respective dimensionless parameters.

Since the above equations are to be solved by the integral method, the basic velocity profile is to be specified by explicitly featuring its radial functional dependence. Considering the asymptotic solutions, it is sought as follows:

$$u(x,r) = u_a(x) (1-r)^{2/\delta(x)} \quad (6)$$

where  $u_a(x)$  and  $\delta(x)$  are two unknown shape functions, turning out to be the velocity on the axis and a measure of the momentum boundary layer thickness, respectively. The group  $\eta = r^{2/\delta(x)}$  can be identified as a similarity variable that incorporates both the axial and radial independent variables.

Satisfying the boundary conditions and the integral mass balance imposes restrictions on the shape functions. In particular, the integral form of the mass balance equation

$$\int_0^1 r u \, dr = 1/2 \quad (7)$$

gives a simple relationship among the two unknown velocity functions:

$$u_a(x) = 1 + \delta(x) \quad (8)$$

To satisfy the boundary condition at the tube entrance, it is required that  $\delta(x \rightarrow 0) = 0$ . The wall and on-axis conditions are satisfied if:  $0 \leq \delta(x) \leq 2$ . As expected, a singular point in the velocity profile occurs for  $x = 0$  and  $r = 1$ . The unknown pressure axial gradient requires a further balance equation.

To this purpose, it seemed convenient to employ the moment method, using the variable  $r^{\delta(x)/4}$  as the weighting function, [26]. The exponent of the power function was chosen to minimize the error in the pressure decay in the inlet region and was determined based on subsequent analysis.

Finally, the two integral balance equations turn out to be:

$$u_r(x,1) = \int_0^1 2r (u^2)_x \, dr + p_x / 2 \quad (9)$$

$$\begin{aligned} \int_0^1 r^{\delta/4} u_r v \, dr + \int_0^1 r^{\delta/4} (u^2)_x / 2 \, dr + p_x \frac{4}{8+\delta} = \\ = \int_0^1 r^{\delta/4} (r u_r)_r \, dr \end{aligned} \quad (10)$$

The subscript 'w' indicates the duct wall, i.e.  $r = 1$ .

The previous set of two equations reveals two unknown functions, i.e. the shape function  $\delta(x)$  and the longitudinal pressure gradient  $p_x(x)$ . Since the first equation is independent of the second, it can be

solved separately to derive an ordinary differential equation for the shape function:

$$\frac{d\delta}{dx} = -2 \frac{(\delta+4)^4 (\delta^2-1) (\delta^3+10\delta^2+24\delta+16)^2}{\delta \cdot f_a(\delta)} \quad (11)$$

$$f_a(\delta) = \delta^9 + 32\delta^8 + 472\delta^7 + 3360\delta^6 + 13248\delta^5 + 38784\delta^4 + 85504\delta^3 + 113664\delta^2 + 73728\delta + 16384$$

By examining this equation, it is immediately evident that the asymptotic solution for the fully developed region is fully recovered when  $\delta(x \rightarrow \infty) = 1$ . Notably, the last equation allows for an immediate implicit solution in the form  $x = x(\delta)$ . Once  $\delta(x)$  is determined, the axial velocity can be derived using Eq. (6). The axial pressure gradient can be obtained through numerical integration of Eq. (10). The radial velocity can be determined by applying the local mass balance, Eq. (1), which results in:

$$v(x,r) = -\frac{r(\delta(x) - r^{2/\delta(x)}(\delta(x) - 2 \log(r)))}{2\delta(x)} \frac{d\delta(x)}{dx} \quad (11')$$

### 3.2 Temperature Field

The dimensionless energy balance equation and the boundary conditions are:

$$r u t_x + r v t_r = (r t_r) / (Pr) \quad (12)$$

$$t(0,r) = 1 \quad (13)$$

$$t_r(x,0) = 0 \quad (14)$$

$$t_r(x,1) = -Bi t(x,1) \quad (15)$$

where:  $t = (T - T_s) / (T_0 - T_s)$ ,  $T_s$  and  $T_0$  being the temperatures of the ambient surrounding the tube and of the fluid at pipe inlet;  $Pr$  is the Prandtl number;  $Bi = (h_{eq} R) / k$  is the Biot number,  $1/h_{eq}$  being the thermal resistance of the wall which includes the resistances of the wall and the tube-ambient, respectively. The limiting case of prescribed wall temperature and wall heat flux are recovered for  $Bi \rightarrow \infty$  and  $Bi \rightarrow 0$ , respectively.

The basic temperature profile is expressed similarly to the velocity profile, i.e. a series expansion in terms of a similarity variable,  $\eta_T = r^{2/\delta_T(x)}$ ,  $\delta_T(x)$  being the temperature shape function, a measure of the temperature boundary layer. By considering the exact solution for fully developed flow with a second-kind boundary condition at the wall, the profile is chosen as follows:

$$t(x,r) = t_w(x) + (t_a(x) - t_w(x)) (1 - \eta_T ((1 - c(x)) \eta_T + c(x))) \quad (16)$$

where  $t_a(x)$  and  $t_w(x)$  are the unknown temperature shape functions, i.e. the temperatures on the axis and at the tube wall, respectively.

Imposing that the approximate solution satisfies the energy balance equation at the collocation point  $r = 1$ , one gets  $c(x) = 4/3$ . This result makes it possible to assert that the exact solution for constant wall heat flux is recovered provided that  $\delta_T(x \rightarrow \infty) = 1$ .

The boundary condition at the wall gives an algebraic relation for the unknown temperature functions:

$$t_a(x) / t_w(x) = 1 + (3/4) Bi \delta_T(x) \quad (17)$$

The boundary condition at the tube entrance gives the initial values for the wall temperature and the shape function:  $\delta_T(x \rightarrow 0) = 0$  and  $t_w(x \rightarrow 0) = 1$ . The assumed temperature profile allows recovering the asymptotic behaviour in the developed temperature region, if  $\delta_T(x \rightarrow \infty)$  reaches a constant value. The two unknown functions,  $\delta_T(x)$  and  $t_w(x)$ , are derived by using two integral equations: the energy balance equation and the energy balance weighted with the temperature similarity variable  $\eta_T$ . The two first-order differential equations are numerically solved by a fourth-order Runge-Kutta scheme.

### 3.3 The FEM Model

In addition to the above, the mass, momentum, and energy equations are solved using commercial CFD software COMSOL Multiphysics v 6.1 along with the associated boundary conditions, [27]. Therefore, a 2D numerical model, FEM based, was developed to simulate heat transfer in simultaneously developing flow and, therefore, to realize a reference useful to verify the accuracy of the approximate solution. A pipe geometry consisting of 1 mm i.d. and 0.6 m long was considered. The domain was discretized using a mapped grid of 152 600 elements. To determine such a result, grid convergence tests were performed using a series of grids with progressively finer resolutions. Temperature error norms were evaluated at selected points, continuing until the errors stabilized and became negligible with further grid refinement. A particularly advantageous feature of the mapped mesh is its excellent control over element size, quality, and growth rate, although it may require additional effort to prescribe the optimal distributions along all edges where geometrical discontinuities make meshing critical.

## 4 Results and Discussion

### 4.1 Behaviour Close to the Tube Inlet

A first way to verify the goodness of the proposed solution consists in comparing it with Blasius' well-known solution close to the tube inlet in the limit  $x \rightarrow 0$ . It is well known from the numerical solution of the Blasius equation that the boundary layer over a semi-infinite flat plate grows as  $4.92 x^{1/2}$ . Taking the limit for  $x$  approaching zero, equation (12) reveals that:  $\delta(x \rightarrow 0) = 4 x^{1/2}$ . Therefore, the well-known Blasius solution's functional dependence is fully recovered and the velocity structure close to the inlet resembles the Leveque boundary layer solution:  $u(x \rightarrow 0, r) = (1/2) (1-r)/x^{1/2}$ .

The thermal solution close to the inlet gives:

$$\begin{aligned} \delta_T(x) &= 2.09 Pr^{-1/3} x^{1/2}; \\ t_w(x) &= 1 - 1.57 Bi Pr^{-1/3} x^{1/2} \end{aligned} \quad (18)$$

As happens for the velocity, the temperature shows a boundary layer behaviour and saves the expected functional dependence on the tube longitudinal coordinate.

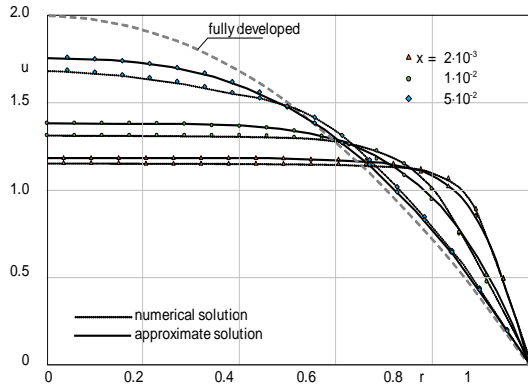


Fig. 1: Developing velocity profiles

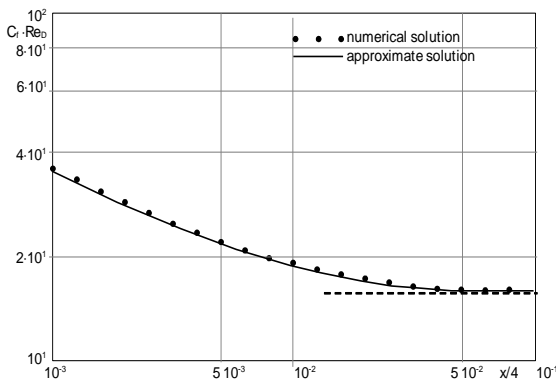


Fig. 2: Local skin friction coefficient

### 4.2 Velocity Field

To show the behaviour of the proposed solution and compare it with the numerical code, the fluid was assumed to be water with constant properties (thermal conductivity  $k = 0.6 \text{ W m}^{-1} \text{ K}^{-1}$ , density  $\rho = 1000 \text{ kg m}^{-3}$ , and dynamic viscosity  $\mu = 8.82 \times 10^{-4} \text{ Pa s}$ ). At the inlet, uniform velocity and temperature of  $0.441 \text{ m/s}$  and  $50^\circ\text{C}$  were assumed, respectively. The outlet pressure was set to 1 bar, while the external fluid temperature and convection coefficient were  $20^\circ\text{C}$  and  $1200 \text{ W m}^{-2} \text{ K}^{-1}$ , respectively. In Figure 1, the developing velocity profiles are reported for selected distances from the inlet. As expected, the slowing down of the fluid due to increasing boundary layer thickness requires that the axial velocity grows along the duct until the fully developed value is recovered. The numerical and the analytical solutions gradually approach each other until they collapse into a single profile in the fully developed region. Here, the above-mentioned occurrence providing  $\delta(x \rightarrow \infty) = 1$  implies the approximated fully developed velocity profile coincides with the exact solution.

Even though the velocities on the axis differ by no more than 6.84% throughout the entire entrance region, it's noteworthy to observe the wall slopes of the approximate and numerical profiles: they appear to exhibit satisfactory agreement. This is significant because the friction between the fluid and the walls is related to the local shear stress at the surface, which is evaluated by the velocity gradient at the wall. Quantitatively, the local skin friction coefficient in the entrance region is presented to characterize the frictional force at the boundary between the fluid and the wall; this dimensionless number is defined as:

$$C_D = \frac{\tau_w}{\rho U_0^2 / 2} = 2 \frac{\left( -\frac{\partial U}{\partial R} \Big|_w \right)}{\rho U_0^2} = \frac{8}{Re} \frac{1 + \delta(x)}{\delta(x)} \quad (19)$$

where  $\tau_w$  is the shear stress at the wall, and  $U_0$  is the characteristic average velocity of the flow over the cross-section. It can be readily checked that the previous structure allows to recover the expected asymptotic value, i.e.  $C_{f,\infty} = 16/Re$ .

The gradual build-up of the fully developed velocity profile from the uniform inlet one is responsible for the curve monotonic decay until the exact asymptotic value is recovered, as shown in Figure 2. Here, the proposed solution is compared with both the numerical solution and the one proposed in [28]. The maximum relative error is contained within the 0.8% in the range under

consideration, which indeed entails a broad operative range.

### 4.3 Temperature Field

The developing temperature profiles depend on the thermal boundary condition at the wall, i.e. on the Biot number, and on the fluid at hand, i.e. on the Prandtl number. In Figure 3, the developing temperature profiles are reported for selected distances from the inlet and compared with the numerical solution, assuming  $Bi = 1$  and  $Pr = 6.15$ . The results obtained from the approximate solution fairly agree with the numerical simulations, with the relative error being less than 1%. This demonstrates that the proposed solution is an effective method for making precise and accurate predictions about the developing temperature field.

The knowledge of the temperature field allows for the calculation of the Nusselt number, which is a critical parameter in heat transfer analysis. In fact, it represents the heat transfer coefficient in a non-dimensional form therefore the wall heat transfer can be calculated.

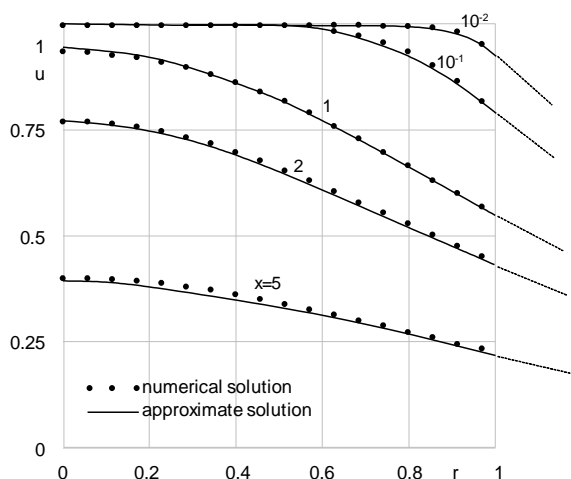


Fig. 3: Developing temperature profiles for  $Pr = 6.15$ ,  $Bi = 1$

A former check for comparing approximate and numerical Nusselt numbers arises from the availability of the well-known Hickman relationship, [22], [29], [30], [31] which applies to the fully developed region (subscript  $\infty$ ):

$$Nu_{\infty}(Bi) = \frac{48/11 + Bi}{1 + Bi/3.66} \quad (20)$$

From this equation, one can derive the limiting cases of uniform wall heat flux, which corresponds to  $Bi = 0$ , and uniform wall temperature, which corresponds to  $Bi = \infty$ . The well-known values for

these cases are 48/11 and 3.66, respectively. For the case at hand featured by  $Bi = 1$ , equation (20) returns  $Nu_{\infty} = 4.21$ . On the other hand, the fully developed Nusselt number can be calculated according to its definition as per equation (16), yielding:

$$Nu_{\infty}(Bi) = -2 \frac{Bi t_w[x \rightarrow \infty]}{t_b[x \rightarrow \infty] - t_w[x \rightarrow \infty]} \quad (21)$$

Evaluating the wall and bulk temperatures as per equation (21) yields a Nusselt number of  $Nu_{\infty} = 4.14$ , resulting in a relative error of 1.6%.

A further validation can be made by evaluating the Hickman relationship for  $Bi \rightarrow 0$  which gives 4.36, fully recovering the approximate value obtained through equation (21). In other words, the structure sought for the approximate temperature profile allows us to completely recover the exact one in the fully developed region. At the other extreme, for  $Bi \rightarrow \infty$ , the error reduces to 0.87%.

the thermal boundary layer thickens along the axial direction, causing the Nusselt number to decrease monotonically along the pipe until it reaches the asymptotic value. The developing Nusselt number, calculated using equation (21) and based on the local temperature values obtained from the approximate solution, is compared with the numerical FEM solution in Figure 4 for the previously selected  $Bi$  and  $Pr$  values. The curves exhibit the anticipated trend, with the relative error decreasing monotonically from 8.6% to 1.6% within the examined range, demonstrating a good agreement between the two methods.

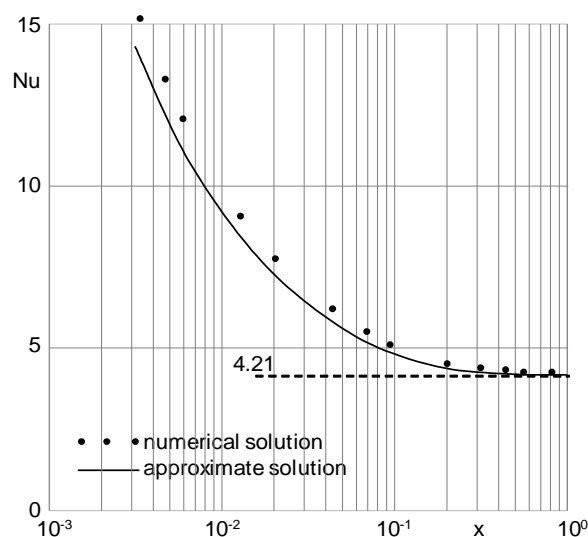


Fig. 4: Nusselt number in the simultaneous entrance region for  $Pr = 6.15$ ,  $Bi = 1$

## 5 Conclusions

In this contribution, the authors demonstrated the validity of an approximate solution for heat transfer in the entrance region of a laminar Newtonian flow in a circular pipe. The main advantages of this innovative approach are the low time and computational cost required when compared to the numerical model. By implementing an integral method to solve the proposed model, interesting results are obtained for both the velocity and temperature profiles.

A comparison of such results with the one obtained with the numerical solutions shows how the proposed model is advantageous since it gives comparable results with significantly lower efforts in terms of both time and computational mess. The relative error for the velocity field is lower than 0.8%, while the relative error for the temperature field is lower than 1%. Such error values are relative to the application of the model at a specific range under consideration, while they increase in exceeding it up to a maximum of 8.6%.

To conclude, the presented model is a valid approximate substitution for FEM methods for a specific range of applications. Future developments will involve the investigation of the solution for a wider range of applications, together with the application of the proposed method to solve heat transfer problem for non-Newtonian flows.

### References:

- [1] T.V. Kármán, On laminar and turbulent friction (Über laminare und turbulente Reibung). *ZAMM-Journal of Applied Mathematics and Mechanics/Zeitschrift für Angewandte Mathematik und Mechanik*, 1(4), 233-252 (1921), <https://doi.org/10.1002/zamm.19210010401>.
- [2] K. Pohlhausen, On the approximate integration of the differential equation of the laminar boundary layer (Zur näherungsweise integration der differentialgleichung der laminaren grenzschicht). *ZAMM-Journal of Applied Mathematics and Mechanics/Zeitschrift für Angewandte Mathematik und Mechanik*, 1(4), 252-290 (1921), <https://doi.org/10.1002/zamm.19210010402>.
- [3] V.A. Kot, Karman–Pohlhausen Method: Critical Analysis and New Solutions for the Boundary Layer on a Plane Plate. *Journal of Engineering Physics and Thermophysics*, 95(4), 1063-1088 (2022). DOI: 10.1007/s10891-022-02570-3.
- [4] A. Becks, J. McNamara, and D. Gaitonde, Linking supersonic boundary layer separation to structural deformation using the Kármán–Pohlhausen momentum-integral equation. *Physics of Fluids*, 34(8) (2022). <https://doi.org/10.1063/5.0101269>.
- [5] Kot, V.A. Polynomial Approximation of the Laminar Boundary Layer on a Flat Plate on the Basis of the Karman Momentum Integral. *Journal of Engineering Physics and Thermophysics*, 96(2), 438-467 (2023).
- [6] Eyo, A. E., Ogbonna, N., Ekpenyong, M. E. Comparison of the exact and approximate values of certain parameters in laminar boundary layer flow using some velocity profiles. *Journal of Mathematics Research*, 4(5), 17 (2012).
- [7] Ajadi, S. O., Adegoke, A., Aziz, A. Slip boundary layer flow of non-Newtonian fluid over a flat plate with convective thermal boundary condition. *International Journal of Nonlinear Science*, 8(3), 300-306 (2009).
- [8] M.M. Metzger and L.C. Klewicki, A comparative study of near-wall turbulence in high and low Reynolds number boundary layers. *Physics of Fluids*, 13(3), 692-701 (2001). <https://doi.org/10.1063/1.1344894>.
- [9] L.P. Erm and P.N. Joubert, Low-Reynolds-number turbulent boundary layers. *Journal of Fluid Mechanics*, 230, 1-44. (1991).
- [10] J.M. Chacin and B.J. Cantwell, Dynamics of a low Reynolds number turbulent boundary layer. *Journal of Fluid Mechanics*, 404, 87-115 (2000). <https://doi.org/10.1017/S002211209900720X>.
- [11] J. Majdalani and L.J. Xuan, On the Kármán momentum-integral approach and the Pohlhausen paradox. *Physics of Fluids*, 32(12) (2020). <https://doi.org/10.1063/5.0036786>.
- [12] J.F. Agassant, P. Avenas, J.Ph. Sergent and P.J. Carreau, *Polymer Processing*, Hanser Publishers (1991)
- [13] C. Rauwendaal *Polymer extrusion*, Hanser Publishers (1986)
- [14] R.K. Shah and A.L. London, Laminar flow forced convection in ducts, *Advances in Heat Transfer*, Academic Press, 153-195 (1978).
- [15] A.H.P. Skelland, *Non-Newtonian Flow and Heat Transfer*, John Wiley & Sons (1967).
- [16] Chhabra, R.P. Non-Newtonian fluids: an introduction. *Rheology of complex fluids*, 3-34 (2010).
- [17] Partal, P., Franco, J.M. Non-newtonian fluids. *Rheology: encyclopaedia of life*

- support systems (EOLSS), UNESCO. *Eolss, Oxford*, 96-119 (2010).
- [18] N. Kushwaha, T.C. Kumawat, K.D.P. Nigam and V. Kumar, Heat transfer and fluid flow characteristics for Newtonian and non-Newtonian fluids in a tube-in-tube helical coil heat exchanger. *Industrial & Engineering Chemistry Research*, 59(9), 3972-3984 (2020).  
<https://dx.doi.org/10.1021/acs.iecr.9b07044>.
- [19] A. Alimoradi and F. Veysi, F Prediction of heat transfer coefficients of shell and coiled tube heat exchangers using numerical method and experimental validation. *International Journal of Thermal Sciences*, 107, 196-208 (2016)  
<https://doi.org/10.1016/j.ijthermalsci.2016.04.010>.
- [20] L.K. Foong, N. Shirani, D. Toghraie, M. Zarringhalam, M. Afrand, Numerical simulation of blood flow inside an artery under applying constant heat flux using Newtonian and non-Newtonian approaches for biomedical engineering, *Computer Methods and Programs in Biomedicine*, 190, 105375 (2020).  
<https://doi.org/10.1016/j.cmpb.2020.105375>.
- [21] R.M. Cotta, *Integral transforms in computational heat and fluid flow*. CRC Press (2020).  
<https://doi.org/10.1201/9781003069065>.
- [22] H.J. Hickman, An Asymptotic Study of the Nusselt-Graetz Problem, Part 1: Large  $x$  Behaviour, *Int. J. Heat and Mass Transfer*, 96, pp. 354-358 (1974).
- [23] T.R. Goodman, *Application of integral method to transient non linear heat transfer*, Ac. Press (1964).
- [24] P.G. Berardi, G. Cuccurullo, Thermal entrance region in fully developed duct flow with viscous dissipation, *Proc. X Congr. Naz. U.I.T.*, Genova, 215-222 (1992).
- [25] P.G. Berardi, G. Cuccurullo, D. Acierno, P. Russo, Viscous dissipation in duct flow of molten polymers, *Proc. Eurother Seminar 46 Heat Transfer in Single Phase Flows*, Pisa, pp. 39-43 (1995).
- [26] P.G. Berardi, G. Cuccurullo, Simultaneously Developing Velocity and Temperature Profiles in Pipe Flow, *Proc. XV Congr. Naz. U.I.T.*, Torino (1997).
- [27] C. Wollblad, *Your Guide to Meshing Techniques for Efficient CFD Modeling*, COMSOL Blog, [Online].  
<https://www.comsol.com/blogs/your-guide-to-meshing-techniques-for-efficient-cfd-modeling>
- [28] A. Bejan, Evolutionary design: Heat and fluid flow together. *International Communications in Heat and Mass Transfer*, 132, 105924 (2022).  
<https://doi.org/10.1016/j.icheatmasstransfer.2022.105924>.
- [29] Tien, C. (1962). Laminar heat transfer of power-law non-Newtonian fluid—the extension of Graet-Nusselt problem. *The Canadian Journal of Chemical Engineering*, 40(3), 130-134.
- [30] Lyche, B. C., & Bird, R. B. (1956). The Graetz-Nusselt problem for a power-law non-Newtonian fluid. *Chemical Engineering Science*, 6(1), 35-41.
- [31] Pnueli, D. (1967). A computation scheme for the asymptotic. Nusselt number in ducts of arbitrary cross-section. *International Journal of Heat and Mass Transfer*, 10(12), 1743-1748.

#### **Contribution of Individual Authors to the Creation of a Scientific Article (Ghostwriting Policy)**

Conceptualization: G. Cuccurullo

Data curation: G. Cuccurullo, C. Concilio, D. Rossi, C. Guarnaccia

Methodology: G. Cuccurullo, C. Concilio

Software: G. Cuccurullo, C. Concilio, D. Rossi, C. Guarnaccia

Supervision: G. Cuccurullo, C. Guarnaccia

Visualization: C. Concilio, D. Rossi

Writing - original draft: G. Cuccurullo, C. Concilio

Writing - review & editing: all the co-authors.

#### **Sources of Funding for Research Presented in a Scientific Article or Scientific Article Itself**

No funding was received for conducting this study.

#### **Conflict of Interest**

The authors have no conflicts of interest to declare.

#### **Creative Commons Attribution License 4.0 (Attribution 4.0 International, CC BY 4.0)**

This article is published under the terms of the Creative Commons Attribution License 4.0

[https://creativecommons.org/licenses/by/4.0/deed.en\\_US](https://creativecommons.org/licenses/by/4.0/deed.en_US)